Interstellar Medium Dynamics and Cosmic Rays Connection to High-Energy Astrophysics

Alexandre Marcowith

Laboratoire Univers et Particules de Montpellier
Alexandre.Marcowith@umontpellier.fr

July 28, 2023

1. Preliminaries
2. Introduction
3. Cosmic Rays: Sources and transport in the interstellar medium
   - Non-thermal phenomena in galactic sources
   - Cosmic-Ray acceleration mechanisms
   - Cosmic-Ray transport theories in the interstellar medium
4. Cosmic-Ray feed back over star formation: large scales
   - Cosmic-ray-driven winds and the role of Streaming instability
   - Multi-fluid approaches to gas dynamics
5. Cosmic-Ray feed back over star formation: small/intermediate scales
   - Low/intermediate energy Cosmic Rays and interstellar medium dynamics
     - Cosmic Ray ionisation
   - Young stars as in-situ sources of Cosmic Rays
6. Perspectives & Conclusions
7. Back-up slides

Table of Contents

All quantities in these lectures are in C.G.S. units

Cosmic Rays and interstellar medium:
M. M. Shapiro, R. Silberberg, J. P. Wefel, 1991, NATO series C, vol 337: Cosmic Rays, Supernovae and the Interstellar Medium [1]
I. Grenier, J.H. Black, A.W. Strong, 2013, ARAA, 53, 199: The nine lives of Cosmic Rays.
M. Padovani et al 2020, SSRv, 216, 29: Impact of Low-Energy Cosmic Rays on Star Formation.
A. Bykov et al 2020, SSRv, 216, 42: High-Energy Particles and Radiation in Star-Forming Regions.
A.Marcowith E.Fermi summer school 2022, foundation of Cosmic Ray physics [2]
Recent CFRCOS4 meeting [3]

Acceleration processes:
L.O'.C. Drury 1983 Reports on Progress in Physics 46 (8), 973 An introduction to the theory of diffusive shock acceleration of energetic particles in tenuous plasmas.
A. Marcowith et al Rev Mod Physics 2016, 79, 046901: The microphysics of collisionless shock waves.

J.Kirk Harbin Lecture (particle acceleration) [4]

[1] https://link.springer.com/book/10.1007/978-94-011-3158-2
[2] https://zenodo.org/record/6735201.YrcEtC8Rr5g
[3] https://u.pcloud.link/publink/show?code=kZqN8IVZSElamY39JfYwtwfPsv76y0onK1gX
[4] https://www.mpi-hd.mpg.de/personalhomes/kirk/publications/Harbin.pdf

Table of Contents

Cosmic Rays ! (CRs)

CRs are energetic non-thermal particles with energies ranging from a few MeV (see Fig. 1) to almost ZeV (10^{21} eV, see Fig 2).
Important point: CRs are mildly-relativistic to relativistic, even if of low number density $\sim 10^{-10}$ cm^{-3} they carry a lot of momenta, energy density/ pressure (see next): in CRs $\underbrace{n_{CR}}_{\text{small}} \times \underbrace{T}_{\text{large = non-thermal}}$, in gas $\underbrace{n_g}_{\text{large}} \times \underbrace{T}_{\text{small=thermal}}$

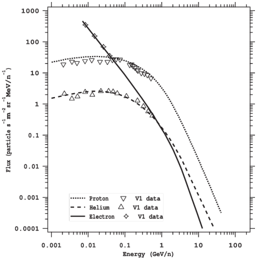

Figure 1: Voyager I Low energy cosmic ray spectrum (Zhang, Xi, Pogorelov, Phys of Plasmas 2015 22 091501, see also Cummings et al 2016 ApJ 831 18). Minimum kinetic energies detected around 3 MeV. Electrons show a very steep spectrum.

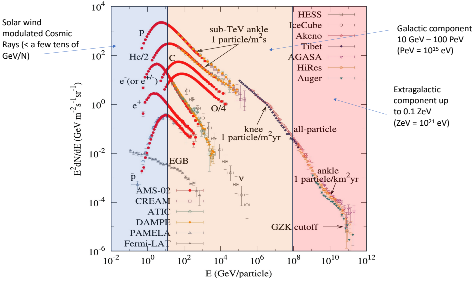

Figure 2: Whole Cosmic Ray spectrum.

One important tool in Cosmic Ray physics: Secondary to Primary ratios

CRs while wandering in the interstellar medium (ISM) have nuclear interaction with matter (H, He) and produce secondary particles through spallation reactions (see Fig. 3, Li/Be/B products of C/N/O interactions).

The ratio of secondary particles (product of spallation) to primary particles can constrain the residence time of CRs in the Galaxy (see next).

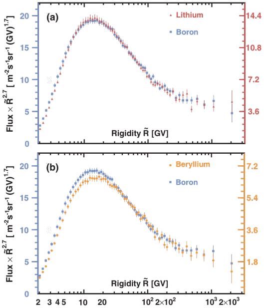

Figure 3: Lithium, Beryllium and Boron spectra in the GeV-TeV range by AMS-02 experiment [Aguilar et al 2018 Phys. Rev. Lett. 120, 021101].

Pressure effects

- **Pressure gradient**: CR pressure gradient is a force in the equation of dynamics (Euler Eq.), [e.g. Dubois et al 2019 A&A 631 A121].

$$\partial_t(\rho\vec{u}) + \vec{\nabla}.\left(\rho\vec{u}\vec{u} + P_{\rm tot}\bar{\bar{I}} - \frac{\vec{B}\vec{B}}{4\pi}\right) = \rho\vec{g} \quad (1)$$

  ρ, $\vec{u}$: gas mass density and velocity, $\vec{B}$ magnetic field, $P_{\rm tot} = P_g + P_m + P_{\rm CR}$, $\vec{g}$: gravitation.

- CRs can modify macro-instabilities relevant to ISM dynamics at various scales: Kelvin-Helmoltz, Rayleigh-Taylor, Magneto-Rotational (accretion), Parker-Jeans (galactic magnetic field dynamo, molecular cloud collapse), Thermal (ISM phases), Firehose/Mirror.
- CRs can produce their own instability: streaming (magnetic field amplification, also due to their current via the Lorentz force $\vec{J} \wedge \vec{B}$), acoustic, Firehose/Mirror.

Why Cosmic Rays are interesting in interstellar medium dynamics studies ? : II ionisation / gas heating

- **Source of ionisation**: Low energy CRs (MeV-GeV: protons, keV-MeV: electrons) can ionise ISM up to high density columns ($> 10^{26}$ cm^{-2}) [Padovani et al 2018 A&A 614 A111].
- **Source of heat**: While ionising they are a strong source of heating [Galli & Padovani 2015 arxiv1502.03380].
- This lecture treats in some details the ionisation process.

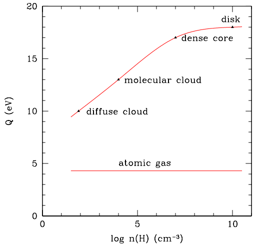

Figure 4: Average heat input per ionisation as function of H density [Galli & Padovani 2015, ibidem, Glassgold et al 2012 ApJ 756 157.]

- **Interaction with atom/molecules/dust**: LECRs interact either directly or through secondary particles (leptons. U.V..) created during interactions [Grenier et al 2015 ARAA 53 199], can have some role in charging/heating dust grains as illustrated in Fig. 5.
- In Ivlev et al 2015 ApJ 812 135: important dust charging process : photoelectric emission induced by secondary U.V. photons produced by H_2 fluorescence $\rightarrow$ affects dust coagulation, medium resistivity ...
- Aspect not treated in this lecture (see references), only impact on CR transport is discussed in backup slide 7.

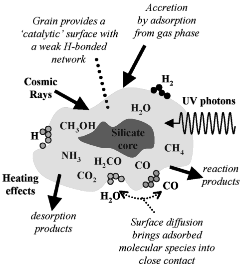

Figure 5: Energetic processes acting on an icy dust in the ISM [Fraser et al 2001 Rev Sci. Instr 73 2161].

The interstellar medium (ISM) is a very complex system of gas, dust, magnetic field and radiation in close interaction. Cosmic Rays are the non-thermal (high energy) component. Among processes injecting energy into the ISM let us cite:

- Instabilities linked to gravitation, rotation, magnetic fields (Magneto-rotational instability, Parker instability, shear motions ...)
- Processes linked with massive star activities: winds, radiation, HII regions expansion, supernova explosion.
- Jets (young stellar objects, X-ray binaries)

Supernova explosions are expected to deposit most of the energy. A simple calculation gives [Mac Low & Klessen 2004 RvMP 76 125]

$$\dot{e}_{\rm SN} = \frac{\sigma_{\rm SN}\eta_{\rm SN}E_{\rm SN}}{\pi R_d^2 H_d} \simeq 3\,10^{-26}\,\frac{\rm erg}{\rm cm^3\ s}\left(\frac{\eta_{\rm SN}}{0.1}\right)\left(\frac{\rm E_{SN}}{10^{51}\ {\rm erg/s}}\right)\left(\frac{\sigma_{\rm SN}}{\rm 1SNu}\right)\left(\frac{\rm H_d}{\rm 100\ pc}\right)^{-1}\left(\frac{\rm R_d}{\rm 20\ kpc}\right)^{-2} \quad (2)$$

$E_{\rm SN}$ is the mechanical energy deposited during a SN explosion, $\eta_{\rm SN}$ is the efficiency of the energy transfer into ISM gas, $\sigma_{\rm SN}$ is the SN rate, with 1 SNu $=$ 1 SN(100 yr^{-1}) $(10^{10} L_B/L_\odot)^{-1}$, where L_B is the blue luminosity of the Galaxy in solar luminosity units, H_d and R_d are the disc height and radius.

- Secondary to primary ratio measurements or radioactive elements abundances $\rightarrow$ GeV CRs stay in our Galaxy for about $t_{\rm res} \simeq 15$ Myears.
  Imparting a fraction of 10% of the energy injected by supernovae into CRs, the CR energy density in the Milky way is

$$\boxed{E_{\rm CR} = 0.1 \times \dot{e}_{\rm SN} \times t_{\rm res} \simeq 1\,\frac{\rm eV}{\rm cm^3}}\,. \tag{3}$$

  CRs are in equipartition with magnetic field and gas energy density in the ISM.

- Supernova explosions with a rate of about 3 events / century are enough to power the CR luminosity in our Galaxy,

$$\boxed{L_{\rm CR} \simeq \frac{E_{\rm CR} V_{\rm CR}}{t_{\rm res}} \simeq 10^{41}\ {\rm erg/s} \left(\frac{\rm V_{CR}}{4\ 10^{67}\ {\rm cm^3}}\right)}\,. \tag{4}$$

  $V_{\rm CR}$ is the galactic volume occupied by CRs.

Note [5].

Main source classes (bold sources discussed during this lecture) and maximum energies (see bibliography for references)

- Supernova (SNe), **Supernova remnants** (SNRs): 0.1-10 PeV (10^{15} eV for protons), possibly the main sources of hadronic (proton/Helium ...) component, gamma-ray emitters.
- **Massive star clusters** (MSCs): 0.1-100 PeV, collective acceleration effects (eg turbulence, multiple shocks ...), gamma-ray emitters.
- Pulsars, pulsar wind nebulae: 1-10 TeV, likely the main sources of leptons (electron/positrons). Around the pulsar itself leptons may be accelerated up to PeV energies. Gamma-ray emitters.
- Compact sources: X-ray binaries, Sgr A*: unknown, possibly contribution to leptons (synchrotron and gamma-ray emitters).
- **Young stellar objects**: Non-thermal electrons are accelerated there (synchrotron radiation from jets), no gamma-rays detected yet (?). Non-thermal radio emission from the magnetospheric activity.

[5] Some sources can inject non-thermal particles but do bot contribute to the CR spectrum

Cosmic Ray spatial scales

A consequence of multiple sources, CRs/EPs can be injected at various ISM scales

- **Massive star clusters**: Injection scale of the bubble (hot, low density medium) around the cluster , hence $L \sim 100 - 300$ pc
- **Supernova remnants**: GeV CRs are likely injected at the merging timescale (SNR shock speed $\sim$ ambient sound speed), so after $10^5 yrs$ over $L = 10 - 100$ pc scales.
- Pulsars, pulsar wind nebulae: $L \sim 10$ pc.
- Compact sources: X-ray binaries, Sgr A*: jet length $L \sim 1$ pc
- **Young stellar objects**: jet length $L \sim 1000$ AU.

CR are injected over multiple scales in the ISM. It is of matter of acceleration models to evaluate the CR luminosity attached to each type of sources.

Table of Contents

Table of Contents

Multi-wavelength non-thermal signatures : Supernova Remnants : synchrotron radio emission

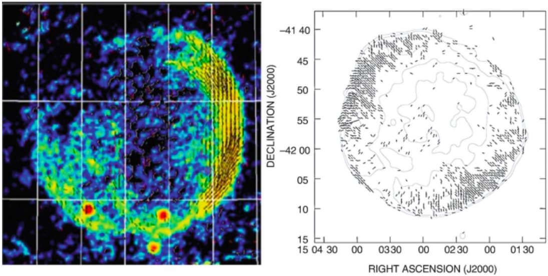

Figure 6: Left : Radio emission from the SNR CTB1 at 10.55 GHz, including polarisation data (lines). Right : Radio emission from SNR 1006 at 1.4 GHz, including polarisation data. From Dubner & Giacani Handbook of Supernovæ 2017, 2041.

Synchrotron radiation marks the presence of GeV electrons. Old SNR have radio magnetic field aligned with the outer shell (CTB1, 7.5-11 kyrs), younger ones have a radial component (SN1006, 1 kyr).

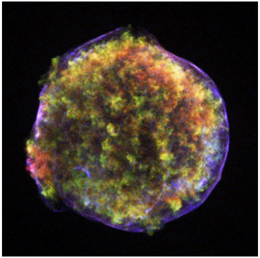

Figure 7: Tycho SNR (discovered by Tycho Brahé in 1572) as detected by the Chandra X-ray satellite (see https://chandra.harvard.edu/photo/2019/tycho/)

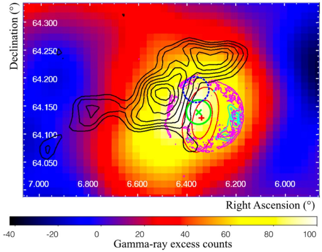

Figure 8: Tycho SNR at TeV [Veritas Cherenkov telescope 2017 ApJ 836 23], Black contours : CO (molecular gas) map, Chandra at 4 keV magenta, NuStar (20-40 keV) in cyan

Young SNRs show evidences of TeV energetic particles production necessary to produce keV X-rays or TeV gamma-rays.

The origin of the the gamma-ray emission is still debated : Inverse-Compton scattering by relativistic electrons (the same producing synchrotron X-rays) and/or neutral pion decay from hadronic interactions.

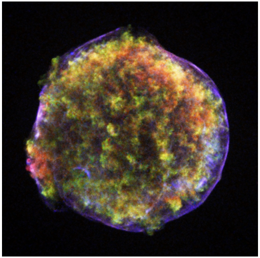

Figure 9: Color codes: red, yellow, green : ejecta (stellar material), blue (4-6 keV): X-ray synchrotron (non-thermal radiation) associated to shock acceleration marked by thin filaments.

The filament size put constraints on the magnetic field strength behind the forward shock.

$$\Delta X_{Fil} \leq Min(\Delta X_{adv}, \Delta X_{dif}) \qquad (5)$$

The advection scale $\Delta X_{adv} = V_{sh} t_{loss}(B)/r$.
The diffusion scale $\Delta X_{dif} \simeq \sqrt{\kappa t_{loss}(B)}$.
V_{sh} the shock speed, κ the particle diffusion coefficient, t_{loss} the synchrotron loss timescale [Parizot et al 2006 453 387]:

$$t_{loss}(B) \simeq 1.25 \times 10^3 \text{ yrs} \left(\frac{\text{E}}{1 \text{ TeV}}\right)^{-1} \left(\frac{\text{B}}{100 \ \mu\text{G}}\right)^{-2} \qquad (6)$$

For Tycho SNR typical values of the magnetic field strength are : 400-500 μG, so *two orders of magnitude above standard ISM values.*

Massive star clusters also show gamma-ray emission at GeV and TeV energies (see Bykov et al 2020 ibid). Below, the example of the Cygnus X region. (but gamma-rays have been detected for Westerlund 1 and 2, the galactic centre region ...)

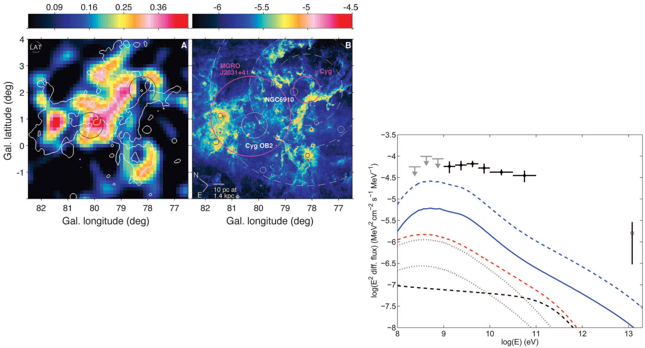

Figure 10: The Cygnus X region. left : Fermi (10-100 GeV) gamma-ray count map , middle: 8 μm map by MSX with the main sources overlaid, right: gamma-ray spectrum [Ackermann et al Science 2011 334 1101]

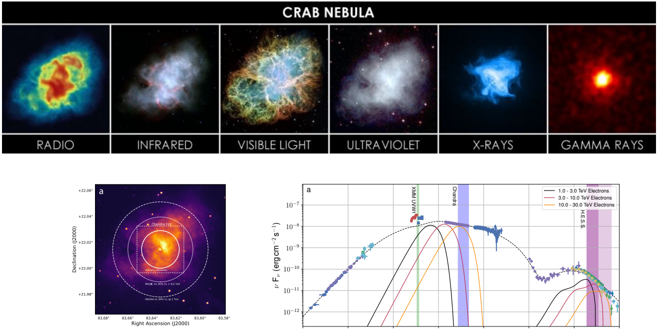

Figure 11: Up: Multiwavelength view of the Crab nebula (1054). Bottom: HESS (High Energy Stereoscopic System) pointing direction (observations 100 GeV-10 TeV). Crab Multi-wavelength spectrum [Hess collaboration Nature Astronomy 2019 4 167]

Electrons (positrons) up to several tens of TeV observed in the Nebula. The Crab nebula is a standard candle in gamma-ray astronomy.

Evolved pulsar gamma-ray halos

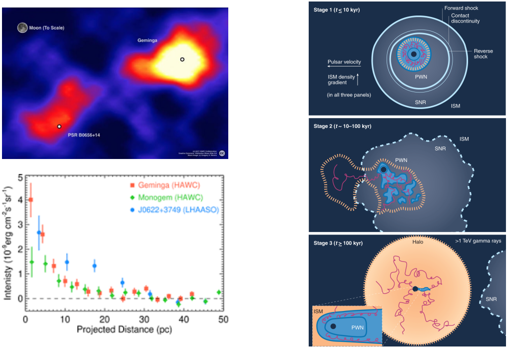

Figure 12: Up-left: Gamma-ray image of GEMINGA and MONOGEM halos by HAWC (above 10 TeV, HAWC website). Bottom-left : Gamma-ray radial profile for three halos [Liu Int Journ Mod Phys A 2022 37 22300011]. Right: sketch of the halo phenomenon.

Gamma-ray profiles can be explained if particles diffuse with a diffusion coefficient reduced by a factor 100-1000 wrt to galactic standards → Cosmic Ray escape problem.

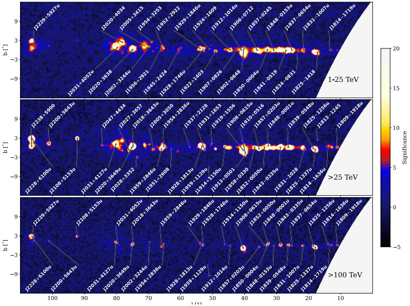

Figure 13: First LHAASO catalogue [Cao et al 2023 ArXiv 2305.17030]. Several sources above 100 TeV are now detected.

Current hot topic : 100 TeV gamma-rays can be produced by protons with energies at 600 TeV (via neutral pion decay) or electrons with similar energies (via Inverse Compton process in the Klein-Nishina regime). No clear counterpart identified yet (several massive star clusters although).

Non-thermal emission in young stellar objects

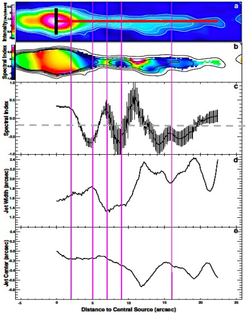

Figure 14: Detailed radio view of the stellar jet from HH8081/IRAS 18162-2048. From up to down: intensity map, spectral index map, spectral index profile, jet width, jet centre poistion [Rodriguez-Kamenetzky et al 2017 ApJ 851 16].

- Young stellar objects are not known to be strong non-thermal sources. Their radio jets are often dominated by thermal free-free radiation [Review by Ray & Ferreira 2021 New Astronomy Reviews 93 101615.].
- Thanks to improved radio sensitivity (u-GMRT, JVLA, LOFAR ...) more objects show non-thermal synchrotron emission [Purser et al 2016 MNRAS 460 1039] both for solar-mass (eg DG Tau [Ainsworth et al 2014 ApJ 792 L18] or massive objects (eg HH8081 [Rodriguez-Kamenetzky et al 2017 ibid]).
- Some hints of gamma-ray emission associated with HH8081 [Yan et al 2022 Research in A&A 22 025016] or S255 NIRS 3 [de Ona Wilhelmi et al 2023 MNRAS 523 105].
- Come back on these sources in part IV.

1. Many types of sources can contribute to the Cosmic Ray spectrum observed on Earth : Supernova remnants, Massive star clusters, pulsar wind nebulae. All show non-thermal emission from radio to gamma-rays (GeV and TeV).
2. X-ray filaments in SNR implies that CR are able to trigger their own instabilities and generate magnetic field at fast shock fronts.
3. Some rare sources should contribute up to PeV energies (LHAASO catalogue).
4. Young stars class shows a growing number of non-thermal radio sources (synchrotron radiation by GeV electrons) and some hints of gamma-rays (see part 4 on small scale feed back)
5. Specific CR propagation seem to be appropriate around sources (eg gamma-ray halos) which show more confinement (wrt to what we should get from standard diffusion regimes, see section on propagation in part 1).

Table of Contents

From Hillas 1984 ARAA 22 425. Criterion fixing the confinement energy of a charged particle (Ze) with an energy E in a region with a magnetic field strength B and size R by imposing (R = Larmor radius of the particle)

$$R = R_L = \frac{E}{ZeB} \text{ or } \log(\mathrm{B}) = -\log(\mathrm{R}) + \log\left(\frac{\mathrm{E}}{\mathrm{Ze}}\right) \text{ see Fig below .} \qquad (7)$$

This is in fact an *upper limit* since for instance losses can limit E further down.

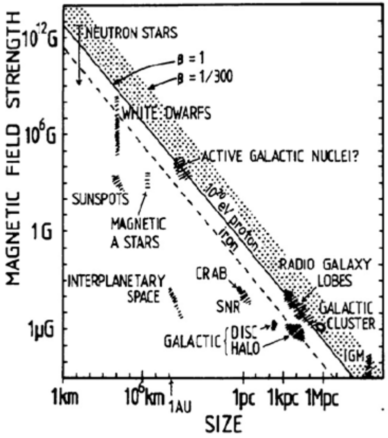

The theory of diffusive shock acceleration : test-particle solution

The main theoretical background dates from late 70s. See review by [Drury 1983 Rep Prog Phys 46 973]. The tenets of the diffusive shock acceleration theory are :

1. Shock: thin discontinuity of thermodynamical quantities (density, gas speed, temperature).
2. Diffusive : up- and downstream the shock front, the gas (plasma + magnetic field) carries electromagnetic perturbations that induce charged particles scattering (because of $\vec{v} \wedge \vec{B}$ force) back and forth the shock front.
3. Acceleration: particles are subject to multiple shock crossings - at each Fermi cycle (eg up-down-up) they gain a constant relative amount of energy.

$$\frac{\Delta E}{E} \simeq \frac{4}{3} \frac{u_1 - u_2}{v} \tag{8}$$

   (v particle speed)
4. Particles have a finite (and small) probability to escape downstream at each cycle because of advection : $\frac{4u_2}{v}$

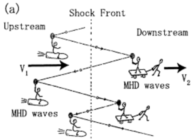

Figure 15: Sketch of the diffusive shock acceleration process in the shock rest frame. u_1 is the gas speed upstream the shock front. $u_2 = u_1 / r$ is the gas speed downstream the shock front. r is the shock or gas mass density compression ratio ρ_2 / ρ_1.

From items (3) and (4) the CR distribution at shock is a power-law $F(E) \propto p^{-(r+2)/(r-1)}$.
Hence $\propto E^{-2}$ for a strong shock, with a sonic Mach number $M_s = u_{sh}/c_{s,1} = u_1/c_{s,1} \gg 1$.

DSA is in fact a *non-linear process* : CRs can back react over the shock solution because of their pressure : they increase the gas compression through *a comsic ray precursor* and modify the value of r [Drury & Voelk 1981 ApJ 248 344]

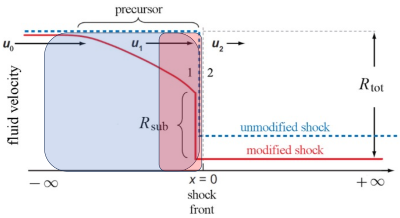

Diffusive length $L(E)= D(E)/u_{sh}$. If two particles have energies $E_1 > E_2$ then $L(E_1)$ (blue) > $L(E_2)$ (red)

Figure 16: Sketch of shock front modified by the presence of CR just ahead (CR precursor). The effective compression ratio of the shock is reduced to a subshock $r_{sub} < r$, but the total (from far upstream to downstream) compression ratio $r_{tot} > r$. Gas compressibility has increased.

The shock solution is not a power-law anymore, it depends on the particle energy [Berezhko & Ellison 1999 ApJ 526 385]

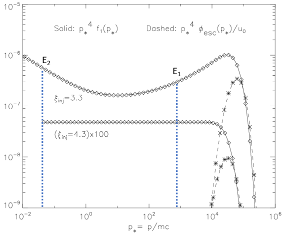

Figure 17: CR spectrum (in momentum) in the test-particle case and in the non-linear case. Low momenta see r_{sub}, high momenta see r_{tot}. At high energy : escaped spectrum at given time or shock radius (from [Caprioli et al 2009 Aph 33 307.]

(illustrative slide) CR are able (via different ways, see next) to produce their own magnetic turbulence they scatter off to proceed with Fermi cycles. They produce *strong magnetic field amplification* ... mandatory to explain X-ray filaments in young SNR.

2D hybrid simulations : electron = fluid, ion =kinetic

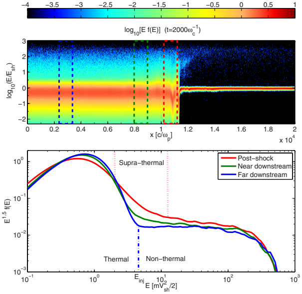

Full 3D particle-in-cell (CR) – MHD (e-i)

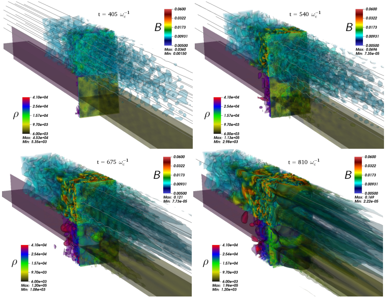

Figure 18: Left: Particle distribution solution accounting for CR and magnetic field back reaction [Caprioli & Spitkovsky 2014 ApJ 783 91]. Right: Magnetic field and gas density evolution in a 3D shock including magnetic field amplification [van Marle et al 2019 MNRAS 490 1156].

Multiple shock acceleration

In the ISM scenarii where CR can interact with multiple shock fronts are not rare.

- Binary systems including one or several massive star (eg Eta Carina).
- Cluster of stars : stellar wind sizes are larger than the mean distances between stars.
- Supersonic ISM turbulence can form multiple shocks.

Basic principle : convolution of one shock solution and re-acceleration [Melrose & Pope 1993 PASA 10 222]. A fully non-linear solution including CR feed back and MFA is still missing.

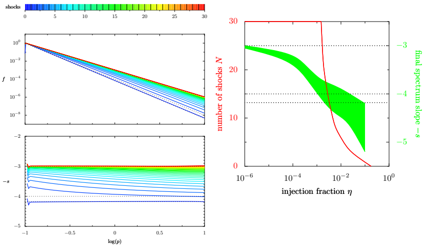

Figure 19: Left : Linear solutions: (up) CR distribution as function of shock number (down) CR distribution spectral index. The asymptotic spectrum scales as p^{-3} or E^{-1}. Right: Non-linear solutions as function of the number of shock and the injection rate: final index distribution in green [G.Ferrand thesis, 2008].

Notice. The injection rate η is the fraction of incoming mass gas flux ρu_{sh} converted into CRs.

1. The standard theory of diffusive shock acceleration predicts a simple solution only dependent on the shock compression ratio r as $F(E) \propto E^{-(r+2)/(r-1)}$ which leads to E^{-2} or p^{-4} for strong shocks.
2. Several non-linear feed back modify this picture: CR carry a huge pressure and increase the gas compression, magnetic field can be strongly amplified by CR themselves. At fast shocks energy densities (gas kinetic, CR and magnetic field respectively) have some typical ordering:

$$
\begin{aligned}
E_{kin} &= \rho u_{sh}^2 \sim \xi E_{CR}, \xi \geq 10 \\
E_{CR} &\sim \frac{c}{u_{sh}} E_B \, .
\end{aligned}
\tag{9}
$$

3. Recent models including magnetic field amplification find that SNR inject a CR distribution scaling $E^{-2.2/-2.4}$ into the ISM at least in the TeV range.
4. GeV CRs (the ones important for ISM dynamics) are rather injected at the end of SNR lifetime with a loosely constrained distribution.
5. Other processes can accelerate CRs , e.g. magnetic reconnection, e.g. [Gaches et al 2021 ApJ, 917, L39] (see part IV).

Table of Contents

CRs are different from the particles part of the background thermal plasma (termed as gas). CRs as energetic charged particles propagate along magnetic field lines at a speed $v = \beta c$ close to c with an helicoidal motion known as Larmor gyration.

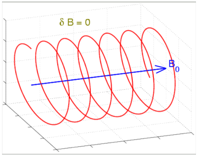

Larmor motion of a charged particle around an uniform magnetic field $\vec{B} = \vec{B}_0$.

- CRs position and momentum respect the Eq of motion

$$\frac{d\vec{x}}{dt} = \vec{v}\,,\, \frac{d\vec{p}}{dt} = q\vec{E} + q\frac{\vec{v}}{c} \wedge \vec{B}\,. \tag{10}$$

- In the ISM $\vec{E}, \vec{B}$ are random variables along the Larmor trajectory. The electric component induces a change in energy whereas the magnetic component induces a change in the pitch-angle $\alpha = (\vec{v}, \vec{B})$.
- α being a random variable modifies the ballistic Larmor motion along $\vec{B}$. CRs while moving close to c can adopt *a random walk along* $\vec{B}$.
- Because 1) CR can jump from one field line to the other and 2) because field lines are turbulent, CRs can adopt *a random walk perpendicular to* $\vec{B}$.

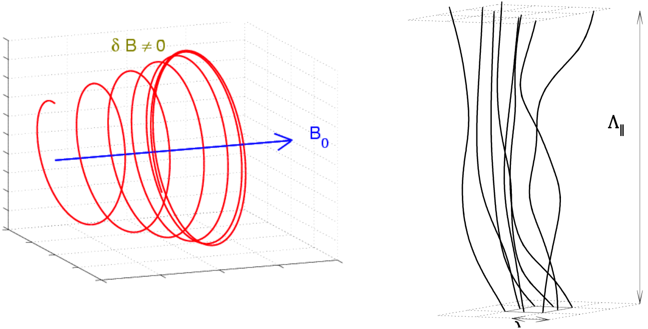

Left: sketch of the particle pitch-angle scattering process due to resonant turbulence-particle interaction. Right : Magnetic field line wandering due to magnetic chaos.

I will consider unless specified particles of modest energies ($E \leq$ TeV), hence a reference gyration radius size is :

$$R_g = \frac{E}{ZeB} \simeq 10^{-3}\,\mathrm{pc}\left(\frac{\mathrm{E}}{\mathrm{TeV}}\right)\left(\frac{\mathrm{B}}{\mu\mathrm{Gauss}}\right)^{-1} \tag{11}$$

Hence $R_g(1\ \mathrm{GeV}) \simeq 5\mathrm{AU}$!!

1. Transport in Large-scale-injected turbulence : The scales of the perturbations have $\lambda > R_g$ or $kR_g < 1$. Turbulence injection scales in the ISM (eg due to supernovae) is $L \sim 10 - 100$ pc.
2. Transport in self-generated turbulence (if it is triggered): The scales of the perturbations can have $kR_g > 1$ (non-resonant) or $kR_g \sim 1$ (resonant) depending on the regime of turbulence.

Nota Bene. These are not golden rules: you may consider *EeV* particles propagating in turbulence of type 1 with $\lambda < R_g$.

In the leaky-box model the diffusion operator in the CR transport Eq. is simplified by an escape process $\nabla D \nabla n_{CR}(E) \rightarrow \frac{n_{CR}(E)}{t_{esc}(E)}$. In a stationary regime, the CR distribution in the ISM $n_{CR}(E)$ is obtained as function of the source injection rate $Q(E)$:

$$n_{CR}(E) = Q(E) t_{esc}(E), \qquad (12)$$

H is the galaxy halo size, mean Hydrogen density is $\langle n_{\rm H} \rangle$, v CR speed

$$t_{esc}(E) \simeq \frac{H^2}{D(E)} = \frac{X(E)}{1.4 m_p \langle n_{\rm H} \rangle v} \qquad (13)$$

B/C ratios give $X(E)$ the *grammage* the amount of matter crossed by a nest of surface of 1 cm^2 carried by CRs. We typically have

$$\boxed{D(E) \simeq 10^{28}\ \mathrm{cm^2/s} \left(\frac{\mathrm{E}}{1\ \mathrm{GeV/N}} \right)^{\alpha}}, \alpha = 0.3...0.6 \qquad (14)$$

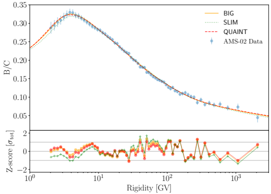

Figure 20: Boron to Carbon abundance ratio in the Cosmic Ray spectrum [Génolini et al 2019 PRD 99 3028]

Quasi-linear theory (QLT) of Cosmic Ray transport

The QLT is the main theory describing the transport of CR in magnetised turbulence [see §A in Casse et al 2001 PRD 65 023002]

There are two main conditions for the QLT to apply:

1. The perturbed fields need to have a small amplitude. Namely $\delta B/B, c\delta E/B \ll 1$.
2. The perturbed fields need to have components displayed over many scales. In other words we need to have a fully developed turbulence.

The theory is effectively applicable in a restricted domain of timescales: $t_c \ll t \ll t_d$, where t_c is the correlation time between stochastic forces and t_d is the timescale of the evolution of the mean particle distribution function.

For instance consider a turbulent spectrum $kW(k) = \frac{\delta B(k)^2}{B^2}$, if a particle undergoes resonant interaction with modes k then $t_c \sim \Omega_s^{-1} k/\Delta k$, Δk is the spectrum width in the parallel MF direction while $t_d \sim \Omega_s^{-1} (B/\delta B)^2$. Hence $t_c \ll t_d$, gives $(\delta B/B)^2 \ll \Delta k/k$, so $\Delta k/k$ can not be too small. Its applicability then depends on the turbulence model (W(k)).

One can show the following results [Schlickeiser 2002 Springer, Shalchi 2009 Springer], see back-up slide 1 for non-linear models.

1. Parallel mean free path $\lambda_{\parallel}$:

$$D_{\parallel}(E) \simeq \frac{1}{3} R_g(E) v(E) \times \frac{B^2}{\delta B(k_{r,\parallel})^2} \rightarrow \lambda_{\parallel}(E) = 3D_{\parallel}(E)/v(E) \qquad (15)$$

The resonant wavenumber is $k_{r,\parallel} \simeq 1/R_g(E)\cos(\alpha)$.
This is the mean distance between two scattering along the magnetic field.
Notice that $\lambda_{\parallel} \propto B^2/\delta B(k_{r,\parallel})^2$. The smaller δB the longer $\lambda_{\parallel}$ (particles are less confined along the magnetic field).

2. Perpendicular mean free path:

$$\lambda_{\perp} \simeq \lambda_{\parallel} \times \frac{\delta B^4}{B^4} \ll \lambda_{\parallel} \, . \qquad (16)$$

[here δB is the total amplitude of magnetic perturbations, $\delta B^2 = \int d\ln(k)\delta B^2(k)$]. In the weak turbulence limit the perpendicular transport is almost negligible wrt to the parallel diffusive transport.

CRs propagate along the mean field line, they tend to produce perturbations with wave perturbations along the mean field line.

Parallel and perpendicular mean free paths in the QLT limit [Shalchi 2009, §3.2.1]: we use a turbulent spectrum $W(k) = W_0(k\ell)^{-\alpha}$ ($k \equiv k_{\|}$). ℓ is the injection scale of the turbulence, $R = R_{\rm g}/\ell$.
The parallel mean free path is given

$$\lambda_{\|} \simeq 3\ell \left(\frac{B}{\delta B}\right)^2 R^{2-\alpha} G(\alpha) \ . \qquad (17)$$

($G(\alpha)$ can be found in Shalchi book)). For resonant slab modes we can use $\alpha = 1$ if the CR distribution scales as $n_{CR}(E) \propto E^{-2}$ (Bohm scaling).
The perpendicular mean free path is given by

$$\lambda_{\perp} \simeq \frac{3}{4} \left(\frac{\delta B}{B}\right)^2 \ell \ . \qquad (18)$$

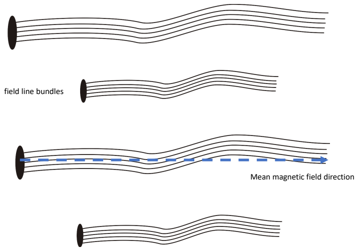

Figure 21: Sketch of slab-type turbulence

A possible source of slab, self-generated perturbations is the (resonant) streaming instability, sketched below. We will come back to it part III about dynamical coupling between CRs and gas. Resonant here means that perturbations are produced at scales corresponding to R_g.

Angular Cosmic Ray distribution

CR anisotropy along B produces a net streaming speed:

$$V_d = \int dp\ v(p) F_{CR}(p) > V_a$$

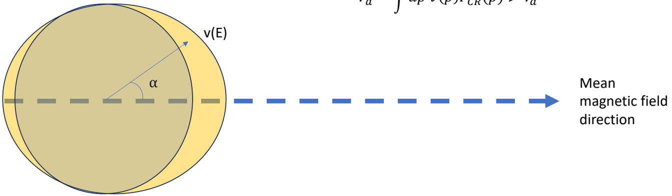

Excess in particle momentum : $\Delta p = \frac{4}{3}\frac{(V_d - V_a)}{c} n_{CR}\langle p \rangle$ transfered to waves $\Delta p = \rho v_a^2 \left(\frac{\delta B}{B}\right)^2$ as CR scatter off perturbations : inelastic scattering between a wave (collective charge motion) and one particle.

Figure 22: A hand waving sketch of the streaming instability

The calculation can be found in : Kulsrud 2005 Princeton University press (Plasma Physics for Astrophysics). See also A. Marcowith lecture on Cosmic-Ray-driven instabilities at Fermi summer school "Foundations of Cosmic Ray Astrophysics", 2022 (in press New Cimento).

The growth rate is [Wiener et al 2013 ApJ 767 87]:

$$\boxed{\Gamma_{CR}(k) = \frac{2\pi m V_a \Omega_c c}{k(\delta B(k))^2} \times \left(-\frac{\partial n_{CR}}{\partial s}\right) A_{CR}} \tag{19}$$

with : $\Omega_c = qB/mc$, m the proton mass, A_{CR} depends on the CR distribution function.

The growth (positive) rate if the gradient of CR density along (along the path s) the magnetic field line is negative - as it is the case for a source of CR which imposes a gradient along B. The growth occurs at a resonant wavenumber $k \sim 1/R_g$.
The Alfvén speed V_a can include neutrals in partially ionised media depending if ions and neutrals are coupled or not.

- The escape process is not completely known, but likely depends on 1) the source evolution stage 2) the CR energy. E.g. in a SNR the highest energies escape first as they have the largest diffusive length $D(E)/v_{\rm sh} = R$ (Hillas criterion).
- Low-energy CRs (below a few tens of GeV) are likely released at the dispersion phase (for a SNR once the shock speed $\sim$ local sound speed).

If the CR energy density in the escaping population is *too low* : they scatter off **large-scale-injected** turbulence after some ballistic regime (moving at c along the background MF).

If the CR energy density in the escaping population is *high enough* : they scatter off **self-generated** turbulence after some ballistic regime (moving at c along the background MF).

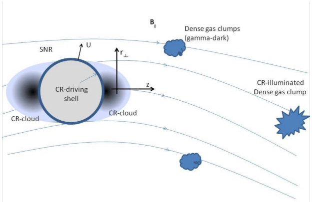

Sketch of the Cosmic Ray Cloud model [Malkov et al 2013 ApJ 768 73] : CR a released along magnetic flux tubes and primarily have a parallel propagation first..

A series of work have investigated this aspect [Malkov et al 2013 ibid, Nava et al 2016 MNRAS 461 3552, Nava et al 2019 MNRAS 484 2684, Brahimi et al 2020 A&A 663 A72, Recchia et al 2022 A&A 660 A57 ...]

The main assumptions :

1. All calculations are 1D. CRs travel along magnetic flux tubes. CR backreaction effects are neglected.
2. The model simultaneously solves two equations: one for CR Pressure - one for wave pressure. The wave are generated by the streaming instability.
3. The diffusion coefficients are calculated in the QLT (see Eq. 15).
4. The model treat CR escape before the remnant dispersion (limited to CR energies above 10 GeV).

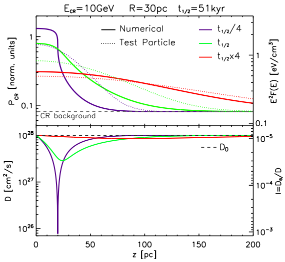

From Nava et al 2016

$t_{1/2}$ is the time after which half of CR have escaped from the SNR.

The reference diffusion coefficient is given by Eq.14.

I(k) is the turbulence amplitude (similar to W(k))

Figure 23: Up: CR pressure (or energy density on right y axis) as function to the SNR distance at three different times. Bottom: CR self-generated diffusion coefficient (or wave amplitude on the right y axis).

CR via self − generated turbulence production can impede their own propagation.

Cosmic Ray transport: a summary

- CR transport is intimately linked to magnetic turbulence properties in the ISM (still loosely constrained).
- Two main turbulent components : Large-scale-injected turbulence / CR self-generated turbulence. The former is likely more effective in CR transport at energies above TeV while the latter one below.
- Even if one average CR pressure is in equilibrium in the ISM, CR sources can inject over pressure by factors 10-100. This injection is very dynamical but can impede the local CR propagation through the streaming instability (for instance).
- Confinement time around sources (eg SNR) varies strongly depending on CR energy (high energy are less confined) and local ISM medium properties (neutrals tend to damp magnetic turbulence and induce less confinement).

Table of Contents

Table of Contents

Figure 24: Left: HST image of NGC 3079 (a) large-scale emission across 15 $\times$ 5 kpc. (b) The 1 $\times$ 1.2 kpc superbubble in H_{α} + [N II] emission. (c) Close-up of the wind-swept, circumnuclear region, X-ray emission is in blue. Right: a kind of extreme object : the starburst galaxy M82 seen in H_{α} (Magenta) [Veilleux 2005 ARAA 43 769]. M82 has a SN explosion rate one order of magnitude larger than our Milky Way.

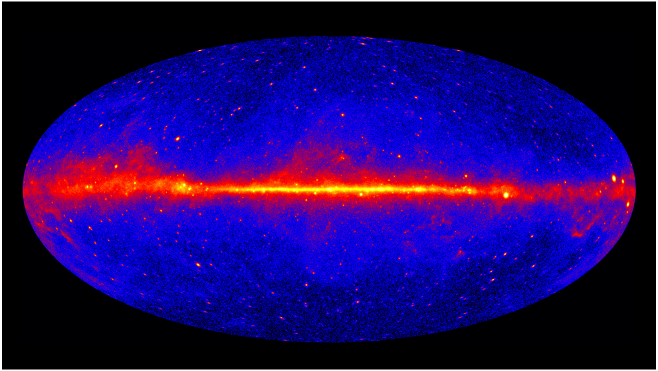

Figure 25: Fermi LAT 60-month image with energies above 1 GeV (credit Nasa).

All CR sources are in the galactic disc : CR pressure support to propel gas into the halo : CR-driven winds.

The advection side of the streaming instability

Important aspect: CR streaming is not only a matter of diffusion but also imposes a relative speed between the gas (magnetised thermal plasma) and CRs. In general, CRs are not advected with the same speed as the gas. The collective CR advection (or streaming) speed is [Skilling 1975 MNRAS 173 255]

$$V_{st} = V_a \times \frac{\nu_+ - \nu_-}{\nu_+ + \nu_-} \ . \tag{20}$$

Here $\nu_\pm$ is the angular scattering frequency of CRs by waves moving either forward (+) or backward (-) along the magnetic field.

1. If CR scatter off large-scale-injected turbulence where one can suppose that the turbulence is balanced, i.e. $\nu_+ = \nu_-$ then $V_{st} = 0$ and CRs have a mean speed equal to the gas speed.
2. If CR scatter off self-generated turbulence one may expect some degree of unbalancing and $V_{st} \neq 0$.

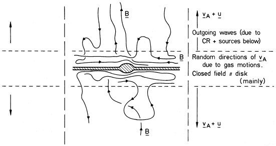

Figure 26: Sketch of the CR driven wind model. In the disc CR move at the same as the gas but as they escape in the halo they trigger the Streaming instability and drive waves moving outward. Momentum is given to the gas as a wind [Breitschwerdt et al 1991 A&A 245 79].

Combined effects of gas, CR and wave (streaming) pressure gradients accelerate the gas and produce a wind.

A long series of work have investigated CR-driven winds : Ipavich 1975 ApJ 196 107, Breitschwerdt et al 1991, Zirakashvili et al 1996 A&A 311 113, Recchia et al 2016 MNRAS 462 L88, Recchia et al 2017 MNRAS 470 865] : all are 1D (flux tube) and stationary.

The model in short

1. Solves a system of magnetohydrodynamic MHD Eqs including CR pressure (see next) + a kinetic Eq for CRs (Fokker-Planck).
2. CR stream at a speed $u + V_a$ and diffuse along the magnetic field with a diffusion coefficient given by Eq. 15. Notice that the bi-fluid models (see next) do not have the kinetic part.

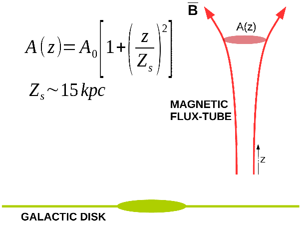

Figure 27: Sketch of the CR driven wind model using a flux tube geometry [Recchia et al 2016 ibid].

Some results

Table 2. Fiducial values for the wind input parameters at the Sun position.

Parameter	Fiducial range
Area-α	1.5–2.0
Area-Z_b	5–15 kpc
Gas density	3–6 $\times$ 10^{-3} cm^{-3}
Gas temperature	1–3 $\times$ 10^6 K
Regular B	1−2 μG
CR pressure	4 $\times$ 10^{-13} erg cm^{-3}

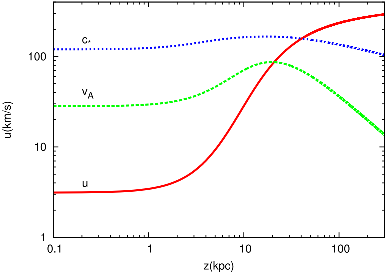

(a) Reference case: velocities.

Figure 28: Left: Fiducial model parameters. Right: Fiducial speeds profile, u is the wind speed [Recchia et al 2017 ibid].

CR driven models produce supersonic wind speed solutions. Set constrains on the CR transport in the galaxy. Connect dark matter halos profiles to the fit of CR local spectrum (see the paper for details).
Can this be tested using numerical simulations ? yes ...

Physical context

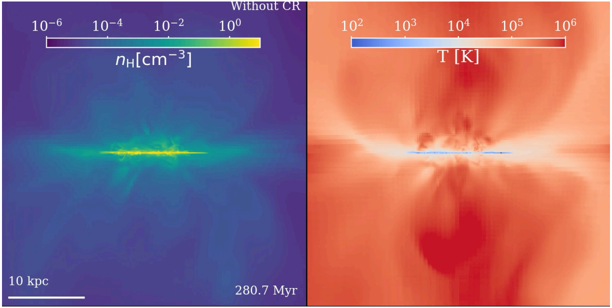

Figure 29: Simulations of outflows for Milky Way-like galaxies including gas, supernova explosion [Farçy et al 2022 MNRAS 513 5000].

Gas outflows are strong regulators of gas content in the disc and hence of star formation (see S.Walch lecture). What is the role of CRs ?

bi-fluid (gas + CRs) Magnetohydrodynamic equations [eg Dubois et al 2019 A&A 631 A121]

$$\frac{\partial \rho}{\partial t} + \nabla.(\rho \boldsymbol{u}) = 0\,,$$ mass

$$\frac{\partial \rho \boldsymbol{u}}{\partial t} + \nabla.\left(\rho \boldsymbol{u}\boldsymbol{u} + P_{\rm tot} - \frac{\boldsymbol{B}\boldsymbol{B}}{4\pi}\right) = 0\,,$$ momentum

$$\frac{\partial e}{\partial t} + \nabla.\left((e + P_{\rm tot})\boldsymbol{u} - \frac{\boldsymbol{B}(\boldsymbol{B}.\boldsymbol{u})}{4\pi}\right) = -\nabla.\boldsymbol{F}_{\rm cond}\,,$$ total energy

$$\frac{\partial \boldsymbol{B}}{\partial t} - \nabla \times (\boldsymbol{u} \times \boldsymbol{B}) = 0\,,$$ magnetic field

$$\frac{\partial e_{\rm CR}}{\partial t} + \nabla.(e_{\rm CR}\boldsymbol{u} + (e_{\rm CR} + P_{\rm CR})\boldsymbol{u}_{\rm st}) = - P_{\rm CR}\nabla.\boldsymbol{u} - \nabla.\boldsymbol{F}_{\rm CR} + \mathcal{L}_{\rm st} + \mathcal{H}_{\rm acc} + \mathcal{L}_{\rm loss}$$ CR energy

System Eqs : one fluid MHD + CR component treated as a fluid through an energy Eq over e_{CR}.

$$\partial_t e_{CR} + \vec{\nabla}.\left(\underbrace{e_{CR}\vec{u}}_{\text{advection}} + \underbrace{(e_{CR} + P_{CR})\vec{V}_{st}}_{\text{streaming}} \right) = -\underbrace{P_{CR}.\vec{\nabla}\vec{u}}_{\text{work}} - \underbrace{\vec{\nabla}.\vec{F}_{CR}}_{\text{diffusion}} + \underbrace{\mathcal{L}_{st}}_{\text{gas streaming heating}} + \underbrace{\mathcal{H}_{acc}}_{\text{shock acceleration}} + \underbrace{\mathcal{L}_{loss}}_{\text{radiative losses}} . \quad (21)$$

Complemented by an Eq for the CR flux:

$$\vec{F}_{CR} = -\underbrace{\bar{\bar{D}}}_{\text{CR diffusion tensor}} .\vec{b}\left(\vec{b}.\vec{\nabla}e_{CR}\right) . \quad (22)$$

Where $\vec{b} = \frac{\vec{B}}{B}$.
The streaming heating term is

$$\mathcal{L}_{st} = -sgn(\vec{b}.\vec{\nabla}e_{CR})\vec{u}_{st}.\vec{\nabla}P_{CR} . \quad (23)$$

More complex models exist : a second moment Eq over the CR flux F_{CR} [Jiang & Oh 2018 ApJ 854 5], Eqs for forward and backward Alfvén wave fluids [Thomas & Pfrommer 2019 MNRAS 498 2977], several population of CRs (different energy bins) [Girichidis et al 2020 MNRAS 491 993], including radiative transfer [Farçy et al 2022 ibid] ...
Remind : CR streaming has three main effects 1) advection of CRs at a different speed wrt to the gas 2) reduces the diffusion coefficient 3) induces gas heating.

- Without CRs (noCR) the wind has several hundred km/s but a low density ($\leq 10^{-3}$ cm^{-3}).
- Diffusion is important to produce fast and dense winds.
- Adding CR pressure only (no diffusion) : wind speed is reduced (SN have more difficulties to inject energy), (not shown in the Fig.).
- Adding Streaming produces stronger winds wrt to no CR case (not shown in the Fig.).

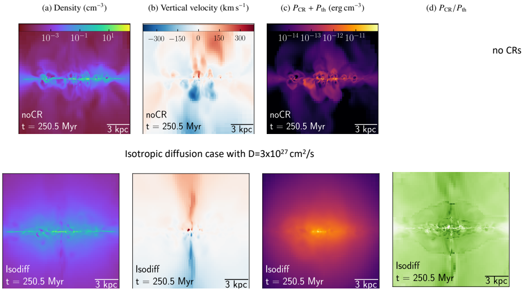

Figure 30: Star formation rate for a galaxy of mass $10^{11} M_\odot$ [Dashyan & Dubois 2020 A&A 638 A123] : a model without CR pressure support and a model with isotropic diffusion.

Cosmic Ray feed back over star formation rate

see recent review by Ruszkowski & Pfrommer ArXiv2306.03141.

- Cosmic Rays regulate the SFR as a negative feed back (a reduction of SFR) because due to the coupling with the gas via the streaming effect they produce denser winds and hence extract more material from the disc (a kind of consensus between simulations).
- The typical amplitude of the feed back is a factor 2 in reduction.
- But the effect is very sensitive to the CR transport assumptions, amplitude of diffusion, anisotropic character ...

Alternative models: suppress CRs around sources → reduces SFR [Semenov et al 2021 ApJ 910 126] - but still not consistent with diffusion associated with Streaming (physics below the grid size).

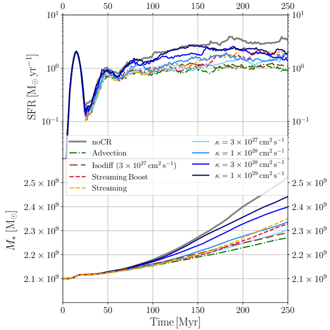

Figure 31: up: Star formation rate for a galaxy of mass $10^{11} M_\odot$ [Dashyan & Dubois 2020 ibid] : different models are : no CR only SN feed back, advection (no streaming $V_{st} = 0$), isodiff = isotropic diffusion (no streaming), streaming boost $V_{st} = fV_a$, f=4 here. Blue lines : anisotropic diffusion $D_\perp = 0.01 D_{||}$. Bottom: stellar mass as a function of time.

- Simulations are now going towards including refined ISM models: including different phases + in some cases radiative transfer [Farçy et al 2022 ibid] ...
- Once the gas distribution is set, and CR energy density is known in the Galaxy-box (simulation box), the gamma-ray emission due to p-p interaction and hence neutral pion decay can be calculated

$$L_\gamma = \underbrace{\int d^3\vec{r}\, n_g(\vec{r}) e_{CR}(\vec{r})}_{\text{gas x CR density}}\, \underbrace{4\pi \int dE_\gamma q_\gamma E_\gamma}_{\text{Gamma-ray emissivity}} \,. \tag{24}$$

- Comparison of different works yield to very different results (see Fig.), why ? more likely the ISM physics (cooling ...).

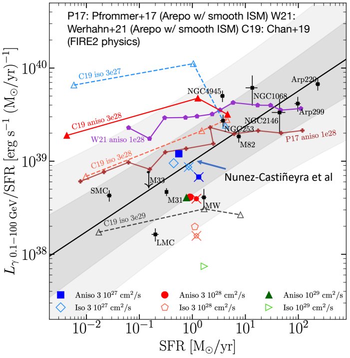

Figure 32: Different 1-10 GeV integrated luminosity issued from different numerical models compared to the Gamma-Ray-Star-Forming-Rate correlation at different galaxy SFR [Nunez-Castieyra et al 2023 sub arXiv:2205.08163].

Table of Contents

Table of Contents

H_2 ionisation rate density column relation

- The derivation of the molecular Hydrogen ionisation rate in different environments (diffuse clouds to dense cores) show 1) a trend of a decreasing ζ with N_{H_2}, 2) Ionization rates higher than the minimum local value [Spitzer & Tomasko] and the one obtained from the local CR spectrum as measured by Voyager probes.
- How to explain such discrepancy ? the low-energy CR (LE-CR) does seem to be highly intermittent, likely because LE-CR sources are intermittently localised in space and time in the ISM.

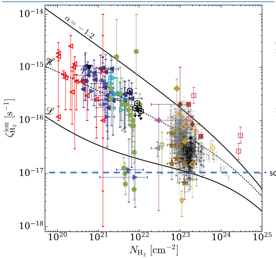

$$j_k^{\rm IS}(E) = C\frac{E^\alpha}{(E+E_0)^\beta}\ {\rm eV^{-1}\ s^{-1}\ cm^{-2}\ sr^{-1}}$$

Table 2. Parameters of the interstellar CR electron and proton spectra, Eq. (2).

Species k	C	E_0 [MeV]	α	$\beta-\alpha$
e	2.1×10^{18}	710	−1.3	3.2
p (model $\mathscr{L}$)	2.4×10^{15}	650	0.1	2.7
p (model $\mathscr{H}$)	2.4×10^{15}	650	−0.8	2.7

Notes. E is in units of MeV and C is in units of ${\rm eV^{-1}\ s^{-1}\ cm^{-2}\ sr^{-1}}$.

Figure 33: H_2 ionisation rate as function of the column density [Padovani et al 2022 A&A 658 A189]. See the article for the references. Three models are plot : $\alpha = -1.2$ and $\mathcal{H}$ fit the diffuse cloud ionisation rates while $\mathcal{L}$ corresponds to Voyager data. Dashed line the lower limit derived by [Spitzer & Tomasko 1968 ApJ 152 971.]

Ionisation rates in active star forming regions

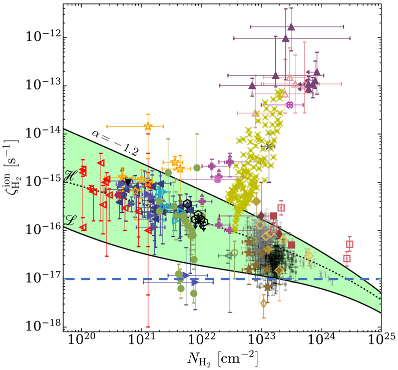

Figure 34: H_2 ionisation rate as function of the column density including data points from star forming regions. Triangles : data from the galactic centre region [Sabatini et al 2023 ApJ 947 L18].

In star forming regions, or close to known CR sources (eg SNR W28) ionisation rates are above $\zeta = 10^{-14}\ \mathrm{s}^{-1}$!

H_2 ionisation rate density column relation : Low energy Cosmic Ray contribution scenarii

We will below review several ways to contribute to ionisation rate enhancements.

- In-situ sources of CRS at intermediate and molecular cloud sizes: HII regions [Padovani et al 2019 A&A 630 A72], Molecular cloud [Gaches et al 2021 ApJ 917 L39], SNR [Vaupré et al 2014 A&A 568 A50].
- Accelerate CRs in sources and hence transport in the ISM: SNR scenario [Jacobs et al 2022 JCAP 05 024, Phan et al 2023 PRD 107 3006], Sagittarus A* [Ravilkularaman in prep], Massive star clusters ....
- Young stars as in-situ sources of CRs [Padovani et al 2016 A&A 590 A8].

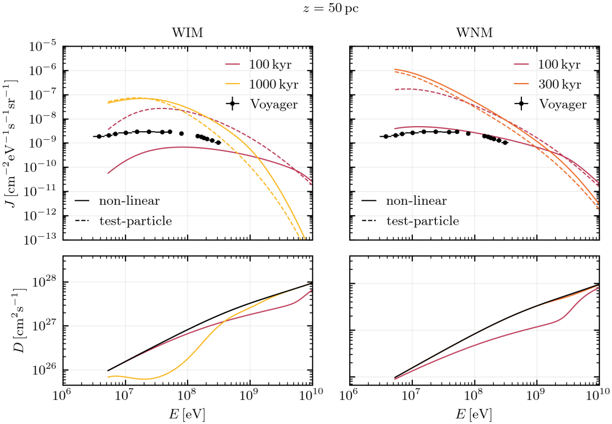

Figure 35: Up: CR propagated spectrum at a distance of 50 pc at different time after escaping the SNR [Jacobs et al 2022 ibid]. Voyager data are displayed in dots. The test-particle solution (propagation is background turbulence) is in dashed lines. The non-linear solution including self-generated turbulence is in continuous line. Down: Diffusion coefficient as function of time and energy. Solid black line: the standard diffusion coefficient as deduced from B/C ratios.

Source injection induces strong CR intermittency at low energies.

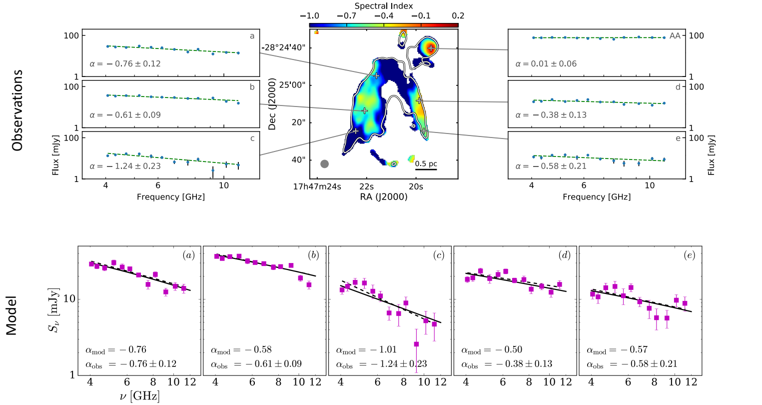

Figure 36: Up: data from Sgr B2(DS) region using the VLA (4-8 GHz band) [Meng et al 2019 A&A 630 A76]. Down: shock model fitting [Padovani et al 2019 ibid].

HII ionisation fronts are associated with shocks which can inject some non-thermal particles (above electrons radiating synchrotron). Local source of non-thermal component hence ionisation (calculation still to be done).

- Tangled gas motions due to (supersonic, superAlfvnic) turbulence in molecular clouds can drive change of magnetic field topology at small scales (ion Larmor radii) $\rightarrow$ magnetic reconnection.
- Energetic particles (either CRs or locally injected) can get accelerated as for a shock by multiple crossings of the reconnection zone.
- A non-thermal distribution with $N(E) \propto E^{-2}$ (here chosen but can be harder [see Drury 2012 MNRAS 422 2474]) which is a strong source of ionisation.

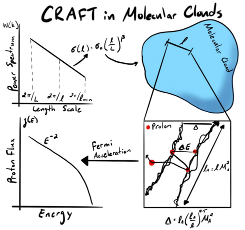

Cloud turbulence =>

magnetic reconnection at small scales =>

Particle acceleration (Fermi I-like) =>

Injection of non-thermal particles in the cloud.

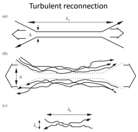

Figure 37: Sketch of the turbulent acceleration model by Gaches et al 2021 ibid. Sketch of the turbulent magnetic reconnection model [Lazarian & Vishniac 1999 ApJ 517 700, Lazarian et al 2013 Phil.Trans.R.Soc.A373:20140144.]

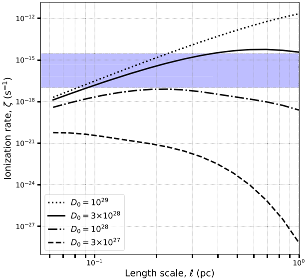

ionisation rates for different diffusion propagation models.

Blue : ionisation rate observed band

Figure 38: Ionisation rate for different diffusion regimes.

Different sites and processes could contribute to accelerate non-thermal particles in young stellar objects.

- At the jet termination shock, more likely at the reverse shock (Mach disc). The external bow shock is suspected to be radiative and likely not a strong non-thermal particle source.
- At internal shocks in the jet either due to non-stationary ejection and/or recollimation effects.
- Near the star either because of the stellar activity (magnetic reconnection, coronal mass ejections) or due to accretion shocks on the stellar surface.

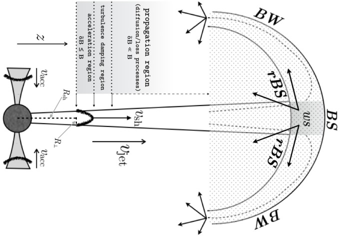

Figure 39: Sketch of acceleration zones in a young stellar objects [Padovani et al 2016, ibid]. Three main sites can be identified : 1) jet termination shock with the ISM (1000-10000 AU scales), internal shocks (100-1000 AU scales), stellar magnetosphere -disc interaction zone (0.01-0.1 AU scales).

It is unknown, let us try an estimate.

1. let us take CR luminosity as a fraction ζ of the jet luminosity $L_{\rm jet} = \dot{M}_{\rm jet} v_{\rm jet}^2$.
2. Jet mass ejection rate $\dot{M}_{\rm jet}$

$$\dot{M}_{\rm jet} = f_w \dot{M}_{\rm acc} \tag{25}$$

   $f_w \sim 0.1$ [Fedriani et al 2019 Nature Communications 10 3630]
3. Jet speed $v_{\rm jet}$

$$v_{\rm jet} = f_K v_K = f_k \sqrt{\frac{GM}{R}} \tag{26}$$

   $f_K \sim 1$ [Federrath et al 2014 ApJ 790 128]
4. all in all:

$$\boxed{L_{\rm CR} \simeq 6\;10^{30}\;{\rm erg/s} \times \frac{\zeta}{0.1} \frac{\rm f_w}{0.1} \left(\frac{\rm f_K}{1}\right)^2 \frac{\rm \dot{M}_{acc}}{10^{-7} M_\odot/yr} \frac{\rm M/M_\odot}{\rm R/0.1AU}}\,. \tag{27}$$

The total luminosity is $L_{\rm CR,tot} = \sum_i L_{\rm CR,i} w_i$, i is the stellar source i in a cluster, w_i is the duty fraction of time where the source is active in injecting CRs. In fine, the luminosity may not be so small. Especially it can contribute to inject CRs at scales ~ 1000 AU.

Put in another way, are YSO jets able to accelerate particles up to GeV-TeV range ? If we base our analysis on diffusive shock acceleration, then the typical maximum energy is fixed by the criterion on the acceleration timescale balancing either escape or radiative losses

$$t_{\rm acc} \simeq f(r)\frac{D(E)}{u_{sh}^2} = Min(t_{\rm esc}, t_{\rm loss}) \ . \quad (28)$$

- It seems that low-mass objects (up to a few solar masses) can not produce energies much beyond GeV [Padovani et al 2016 ibid]
- Massive YSO have faster jet (and shock) speeds, eg HH80-81 have $v_j \sim 1000$ km/s then the acceleration time drops (see Eq. 28) and multi-hundreds - TeV energies may be reached [Araudo et al 2021 MNRAS 504 2405].
- Actually the detection of single sources is difficult, but the collective contribution of massive star cluster could be detectable (under progess).

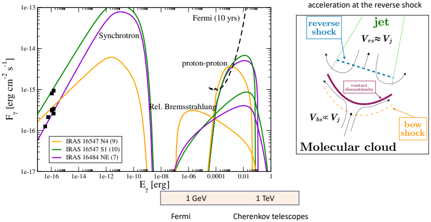

Figure 40: Right: multi-wavelength spectra for three massive YSO. The gamma-ray range is sketched in the orange box. The model considers only the acceleration at the reverse ending shock of the jet [Araudo et al 2021 ibdi].

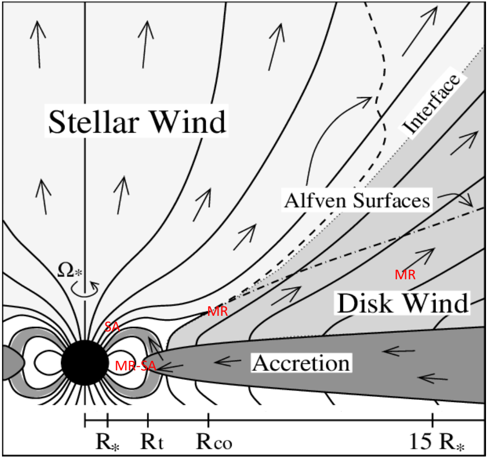

In-situ Energetic particle acceleration sites
MR = Magnetic reconnection
Shock acceleration = SA

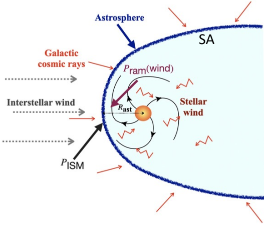

Cosmic Ray modulation by the Astrosphere

Figure 41: Sketch of particle acceleration sites in TTauri-like objects. On right sketch of an Astrosphere which modulates background Cosmic Rays because of the wind

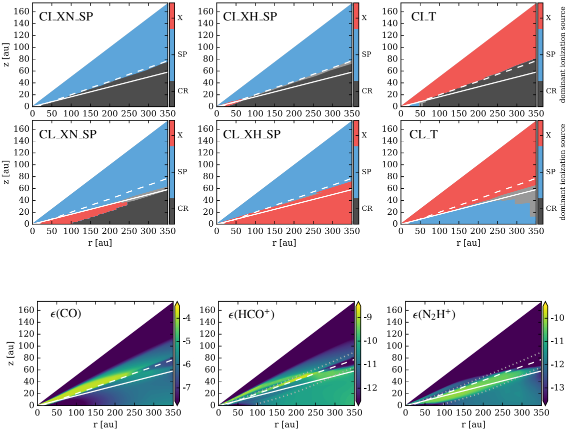

Models

Name	X-rays	Stellar particles	Cosmic rays
CI_XN	normal[a]	–	ISM[d]
CI_XH	high[b]	–	ISM
CI_XN_SP	normal	active T Tauri	ISM
CI_XH_SP	high	active T Tauri	ISM
CI_T	Turner[c]	Turner	ISM
CL_XN	normal	–	low[e]
CL_XH	high	–	low
CL_XN_SP	normal	active T Tauri	low
CL_XH_SP	high	active T Tauri	low
CL_T	Turner	Turner	low

Figure 42: Main sources of disc ionisation for different models (see the table) between X-rays, Cosmic-Rays and in-situ accelerated energetic particles. Three species abundances calculated using the PRODIMO code for model CI_XN [Rab et al 2017 A&A 603 A96].

In-situ accelerated energetic particles can impact the disc local ionisation rate deeply [Brunn et al 2023 MNRAS 519 5673, Kimura et al 2023 ApJ 944 192].

Cosmic Rays are important as many aspects of the ISM dynamics over different scales by different means

- Means : current, pressure gradient (= force), ionisation at high density columns, spallation (production of nuclear elements like Lithium, not covered by the lecture, see Tatischeff & Gabici 2018 Annual Review of Nuclear and Particle Science 68 377).
- Scales : Large (kpc) = regulate SFR via winds, partly control magnetic field dynamo (Parker instability, not covered, see back-up slide 2), Medium (pc-100 pc) = regulate the thermal instability (phase equilibrium, not covered) also via streaming heating effect, nearby source ISM dynamics, dust interaction (not covered, back-up slide 6), H_2 ionisation in molecular clouds hence gas-magnetic field coupling, Small (AU-0.01 pc) = ionisation in jets, accretion disc ionisation (so the control of MRI).
- some complementary reviews : Cosmogenic studies [David & Leya 2019 Progress in Particle and Nuclear Physics 109 103711], Spallogenic Nucleosynthesis [Tatischeff & Gabici 2018 ibid].

Some hot topics :

- Cosmic Ray feed back : inclusion of feed back channels : streaming but other instabilities can be important (eg firehose).
- Dust studies : covers a wide domain from laboratory experiments to theoretical studies. (back up slide 7)
- Source-scale dynamics and their inclusion in SFR calculations (modified supernova feed back). What is the role of massive star cluster in Cosmic Ray feed back ?
- Young stars and in-situ sources of energetic particles as a small scale feed back channel.
- Feed back over planetary atmospheres and life (see ETERNAL ISSI team https://www.issibern.ch/teams/exoeternal/)
- A relatively new subject - so there are rooms for PhD thesis and/or Postdoc if you are interested in.

Table of Contents

The quasi-linear theory is only the simplest microscopic theory to describe CR propagation. But it has severe drawbacks, in particular it describes wave-particle interaction by mean of resonance. Its resonant kernel has the form of a Dirac peak:

$$R(\vec{k},\omega) = \delta(k_{\parallel} v_{\parallel} - \omega \pm \Omega_s) \tag{29}$$

In the MHD regime (low frequency waves $\omega \ll \Omega_s$) this reduces to $\delta(k_{\parallel} v_{\parallel} \pm \Omega_s)$ or shortly

$$r_g = \frac{1}{k\eta\mu}, \mu = \cos\left(\vec{v},\vec{B}\right), \eta = \cos\left(\vec{k},\vec{B}\right) , \tag{30}$$

It is clear that as $\mu \to 0$ one need $k \to \infty$, one needs very small wavelength perturbations to ensure scattering. Never the case in reality.

The object of non-linear theories is mainly to treat this pathological behavior by changing the Dirac peak to another function (eg Lorentzian). It is described in Shalchi 2009 Non-Linear Cosmic Ray diffusion theories, Springer.

Cosmic Rays because of their pressure gradient impulse a force over the magnetised gas. If their diffusion coefficient is not too large, CRs are coupled to the gas for an amount of time long enough to compete with standard macro-instability growth rates. Below a couple of references for diverse instabilities.

- Kelvin-Helmoltz instability [Suzuki et al 2014 ApJ 787 169]
- Magneto-Rotational Instability [Kuwabara & Ko 2006 ApJ 636 290]
- Parker-Jeans instability [Shadmehri 2009 MNRAS 397 1521]
- Rayleigh-Taylor instability [Ryu et al 1993 ApJ 405 199]
- Mirror / Firehose instabilities [Osipov et al 2017 Journal of Physics Conference Series. 929 012006]
- Streaming non-resonant instability [Bell 2004 MNRAS 353 550]
- Acoustic Instability [Drury 1984 Adv Space Research 4 185]

Low energy CRs (the ones important for ISM dynamics, ionisation, spallation ...) have a very small Larmor radius, hence diffusion coefficient (if they diffuse at all). In order to describe this diffusion process properly one needs to have a numerical time step (in explicit schemes) defined as

$$\Delta t = \frac{\Delta x^2}{2D(E)} \ . \tag{31}$$

High resolution (small Δx) are necessary to keep reasonable time steps. Diverse techniques can be used as a cure, see [Dubois & Commerçon 2016 A&A 585 A138].

The self-generated diffusion coefficients are also dependent on the local values of ∇P_{CR} and they may be fixed by setting $\Gamma_g = \Gamma_d$ where $\Gamma_{g/d}$ are the streaming instability growth rate and the damping rate respectively [Commerçon et al 2019 A&A 622 A143, Nunez-Castieyra et al 2023 sub arXiv:2205.08163].

Intermezzo - an intermediary-scale dynamical effect : supernova remnant momentum thrust

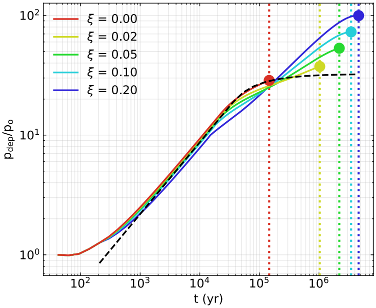

Analytical thin-shell approximation

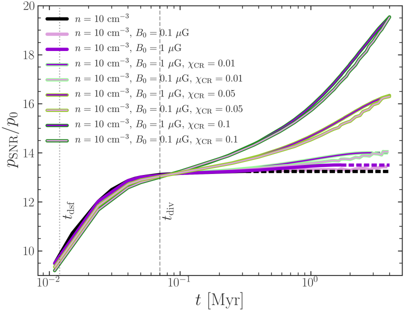

bi-fluid MHD simulations using RAMSES code.

Figure 43: Left : Momentum-time deposition by a SNR as function of the CR content (ζ = fraction of incoming flux imparted into CRs) [Diesing & Caprioli 2018 PRL 121 091101], the dots mark the end point of the SNR life time. Right: The same but using a bi-fluid approach [Rodriguez-Montero et al 2022 MNRAS 511 1247]

Typical momentum gain by a factor of a few if CR are included.

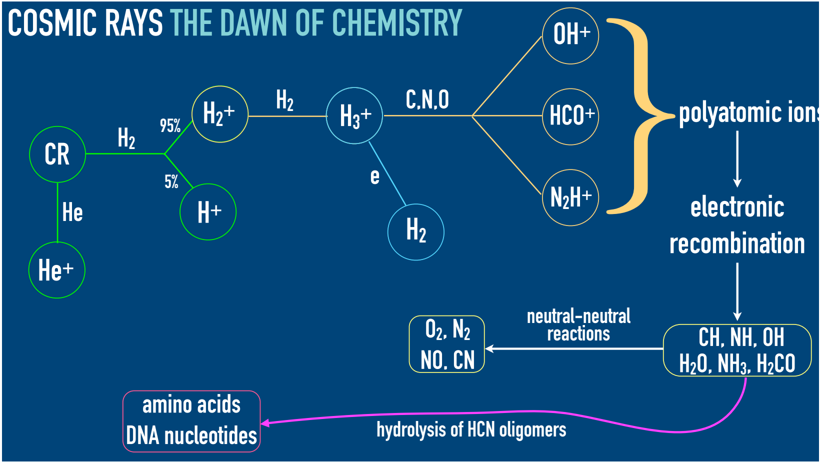

Figure 44: Main chemical network induced by CRs [Padovani 2023, CFRCOS4 presentation, see preliminaries slide]

CR secondaries ionisation at high column densities

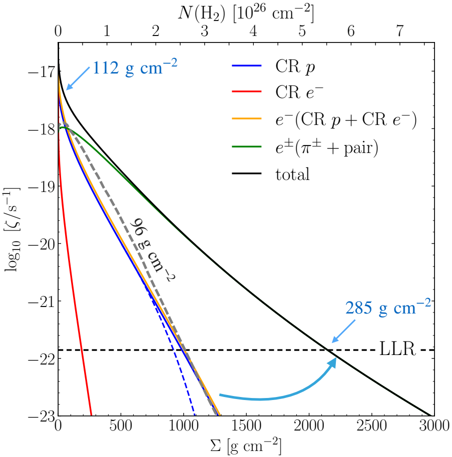

Figure 45: Ionisation rates at high-column densities (above 10^{26} cm^{-2}). The ionisation is dominated by electron-positron secondaries produced by charged pion decay (high energy proton only) [Padovani et al 2018 A&A 614 A111]. LLR = ground ionisation rate produced by Long Live Radioactive nuclei.

Cosmic Rays and dust studies

CRs have an impact over grains (see slide 10 and references therein) but recent studies point towards a feed back of dust on CR propagation [Squire et al 2020 MNRAS 502 2630].

- Dust can have opposite feed back over CR transport either 1) enhancing the transport because of CR self-generated waves damping 2) a confining effect by contributing to slab wave growth. The main parameter controlling the correct regime is the drift speed of the dust $v_{d,g}$
- If $v_{d,g} < V_a = B/\sqrt{4\pi\rho}$: Alfvén waves are damped and CR transport enhanced. (ρ is the gas mass density, one fluid model proposed in this model)
- If $v_{d,g} > V_a$: Alfvén waves are produced and CR are more confined.

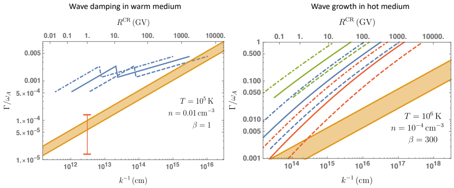

Figure 46: Left: slab wave damping ($\Gamma < 0$) in warm medium : (yellow zone): turbulent damping, (red) : Non-linear Landau damping, (blue) dust damping (for different dust charge). Right : similar plot but showing wave growth ($\Gamma > 0$) in hot medium.